ACTA MECHANICA
Acta Mechanica 2004 *July 6, 2004*

COUPLED ANALYSIS OF COMPOSITE LAMINATE WITH MAGNETOSTRICTIVE ACTUATOR AND SENSOR.

D. P. Ghosh, S. Gopalakrishnan*

Department of Aerospace Engineering, Indian Institute of Science, Bangalore 560012, India.

KEY WORDS: Magnetostrictive, Magneto-mechanical Coupling, FEM.

1. INTRODUCTION

Composites have revolutionized structural construction. They are extensively used in aerospace, civil , mechanical and other industries. Present day aerospace vehicles have composites up to 60% or more of the total material used. More recently, materials which can give rise to mechanical response when subjected to non-mechanical loads such as PZTs, magnetostrictive, SMAs, have become available. Such materials may broadly referred to as functional materials. With the availability of functional materials and the feasibility of embedding them into or bonding them to composite structures, smart structural concepts are emerging to be attractive for potential high performance structural applications [1]. A smart structure may be generally defined as one which has the ability to determine its current state, decides in a rational manner on a set of actions that would change its state to a more desirable state and carries out these actions in a controlled manner in a short period of time. With such features incorporated in a structure by embedding functional materials, it is feasible to achieve technological advances such as vibration and noise reduction, high pointing accuracy of antennae, damage detection, damage mitigation etc. [2, 3].

Some magnetic materials (magnetostrictive) show elongation and contraction in the magnetization direction due to an induced magnetic field. This is called the magnetostriction, which is due to the switching of a large amount of magnetic domains caused by spontaneous magnetization, below the Curie point of temperature. These magnetostrictive materials have the ability to convert magnetic energy into mechanical energy and vice versa. This coupling between magnetic and mechanical energies represents the transudation capability that allows a magnetostrictive material to be used in both actuation and sensing devices. Due to

*Correspondence to: Dr. S. Gopalakrishnan, E-mail: krishnan@aero.iisc.ernet.in, Tel: +91 080 22932757, Fax: +91 080 3600134

magnetostriction and its inverse effect (also called Villery effect)[4], magnetostrictive materials can be used both as an actuator and as well as a sensor.

The theoretical and experimental study of magnetostrictive materials has been the focus of considerable research for many years. However, only with the recent development of giant magnetostrictive materials (e.g. Terfenol-D), it is now possible to produce sufficiently large strains and forces to facilitate the use of these materials in actuators and sensors. This has led to the application of magnetostrictive materials to such devices as micro-positioners, vibration controller, sonar projectors and insulators, etc. Magnetostrictive material has found its way in many structural application such as vibration control, noise control and structural health monitoring.

Non-contact magnetostrictive strain sensor was explored by Kleinke, et al. [5] and the study of magnetostrictive particulate actuator was done by Anjanappa, et al. [6]. The use of this material in smart laminated composites for vibration suppression, is examined by many researchers. Reddy and Barbosa [7] investigated laminated composite beams and Lee et al. for composite plate [8] containing magnetostrictive layers modelled as distributed parameter systems to control the vibration suppression. The effect of material properties, lamination scheme, and placement of the magnetostrictive layers on vibration suppression were investigated. Nakamura et. al. [9] developed an active six degrees-of-freedom micro-vibration control system using giant magnetostrictive actuators. Pelinescu and Balachandran [10] presented analytical investigations conducted into active control of longitudinal and flexural vibrations transmitted through a cylindrical strut fitted with piezoelectric and magnetostrictive actuators. Mahapatra et al. [11] have used this material to suppress all the frequency gear box noise components for active noise control in helicopter passenger cabin. Fenn et. al. [12] developed a vibration reduction system for the UH-60A helicopter using magnetostrictive actuators drive with four trailing edge flaps on each blade. Anjanappa and Bi [13], developed an integrated model to analyze the vibration suppression capability of a cantilever beam embedded with magnetostrictive mini actuator using the Euler-Bernoulli beam theory and strain energy conservation principle. Qian et. al. [14] investigated vibration control for simply supported laminated composite shells with smart plies acting as sensor and actuator layers through magnetostrictive actuation. Brennan et. al. [15] demonstrated the practical viability of a non-intrusive magnetostrictive actuator and sensor for the active control of fluid-waves in a pipe. Sensing of delamination in composite laminates using embedded magnetostrictive material was studied by Krishna Murty, et al. [16]. Saida et. al. [17] experimentally demonstrated the use of this material for structural health monitoring of composite beams.

Analysis of smart structures using magnetostrictive materials are generally performed using uncoupled models. Uncoupled models are based on the assumption that the magnetic field within the magnetostrictive material is proportional to the electric coil current times the number of coil turn per unit length [18]. And due to this assumption, actuation and sensing equations gets uncoupled. Where, for actuator, strain due to magnetic field (which is proportional to coil current) is incorporated as the equivalent nodal load in the finite element model for calculating the block force due to this strain. Thus, using this assumption, analysis of smart structure are carried out without having smart (magnetic field) degrees of freedom in the finite element model. Similarly for sensor, where generally coil current is zero, the magnetic flux density is proportional to mechanical stress, which can be calculated from the finite element results as a post-processor. This assumption on the magnetic field, leads to the violation of flux line continuity, which is one of the four Maxwell's equations in electromagnetism.

In the case of coupled model, it is considered that magnetic flux density and/or strain of the material are functions of stress and magnetic field, without any additional assumption on magnetic field. Benbouzid et al. modelled the static [20] and dynamic [21] behavior of the nonlinear magneto-elastic medium for magneto-static case using finite element method. Magneto-mechanical coupling was incorporated considering both permeability and elastic modulus as functions of stress and magnetic field. In reference [22], finite elements were used for modelling different magnetic circuits with leakage flux of a basic actuator configuration. However, none has provided a convenient way for analysis of magnetostrictive smart structure considering coupled magneto-mechanical features. In this work we presented a new finite element formulation for structures with in-built magnetostrictive patches, that can handle coupled analysis. Here, both magnetic and mechanical degrees are considered as unknown degrees of freedom. In the present approach, smart patches are introduced in the laminates to induce actuation strains and to hence the stress condition. The application of magnetic field to the actuating patch introduces strain in the embedded magnetostrictive patch. This changes state of stress in the sensing patch and so magnetic flux density through enclosed magnetic coil changes, resulting in a voltage across the sensing coil.

This paper is organized as follows. First the variational formulation is illustrated to get the mass, stiffness and coupling stiffness of the system. The paper is then concluded with some specific remarks. In this paper a numerical study on 12 layered beam containing two patches, one acting as an actuator and the other as a sensor has been presented.

2. CONSTITUTIVE MODEL FOR MAGNETOSTRICTIVE MATERIAL

Application of magnetic field causes strain (magnetostriction) in the magnetostrictive material (Terfenol-D) and hence the stress, which changes magnetic flux density of that material [23]. The three-dimensional constitutive relationship for magnetostrictive material is generally written as

$$\{\epsilon\} = [S^{(H)}]\{\sigma\} + [d]^T\{H\} \tag{1}$$

$$\{B\} = [d]\{\sigma\} + [\mu^{(\sigma)}]\{H\} \tag{2}$$

where $\{\epsilon\}$ and $\{\sigma\}$ are strain and stress respectively. $[\mathbf{S^{(H)}}]$ represents elastic compliance measured at constant $\mathbf{\{H\}}$ and $[\mu^{(\sigma)}]$ represents the permeability measured at constant stress $\{\sigma\}$. Here $\mathbf{[d]}$ is the magneto-mechanical strain coefficient, which provides a measure of the coupling between the mechanical strain and magnetic field. For ordinary material where the magneto-mechanical strain coefficient is zero, Equation-1 comes to generalized hooks law and Equation-2 comes to constitutive equation of magnetic material. In general, $[\mathbf{S}]$, $[\mathbf{d}]$ and $[\mu]$ are nonlinear as they depend upon $\{\sigma\}$ and $\{\mathbf{H}\}$. However, reasonable response estimation can be obtained by treating them as linear [23]. Hence, in this analysis, we consider the linearized constitutive relation.

To work with displacement based finite element formulation, above equations were rewritten as

$$\{\sigma\} = [Q]\{\epsilon\} - [e]^T\{H\} \tag{3}$$

$$\{B\} = [e]\{\epsilon\} + [\mu^{\epsilon}]\{H\} \tag{4}$$

Where [**Q**] is Elasticity matrix, inverse of compliance matrix [**S**], $[\mu^\epsilon]$ is the permeability matrix at constant strain and [**e**] is magneto-mechanical stress coefficient matrix. [**e**] and $[\mu^\epsilon]$ are related to [**Q**] through

$$[e] = [d][Q] \tag{5}$$

$$[\mu^\epsilon] = [\mu^\sigma] - [d][Q][d]^T \tag{6}$$

For ordinary magnetic materials, where magneto-mechanical strain coefficients are zero, $[\mu^\epsilon]$=$[\mu^\sigma]$, the permeability.

3. GENERAL 3-D FINITE ELEMENT FORMULATION

Finite element formulation begins by writing the associated energy in terms of nodal degrees of freedom by assuming the displacement and magnetic field variation over each element. That displacement field $\{U\}$ can be written as

$$U = \begin{Bmatrix} u \\ v \\ w \end{Bmatrix} \tag{7}$$

where $u(x, y, z, t), v(x, y, z, t)$ and $w(x, y, z, t)$ are the displacement component in x, y and z direction respectively. These displacements are obtained from element nodal displacements $\{U^e(t)\}$, through the shape function, $[N_U(x, y, z)]$ as

$$\{U\} = [N_U]\{U^e\} \tag{8}$$

To get the strain ϵ in terms of displacement $\{U\}$, differential operator $[L]$ on displacement field $\{U\}$ are used as

$$\{\epsilon\} = \{\epsilon_{xx} \;\; \epsilon_{yy} \;\; \epsilon_{zz} \;\; \gamma_{yz} \;\; \gamma_{xz} \;\; \gamma_{xy} \;\}^T = [L]\{U\} \tag{9}$$

Where L is

$$[L] = \begin{bmatrix} \frac{\partial}{\partial x} & 0 & 0 \\ 0 & \frac{\partial}{\partial y} & 0 \\ 0 & 0 & \frac{\partial}{\partial z} \\ 0 & \frac{\partial}{\partial z} & \frac{\partial}{\partial y} \\ \frac{\partial}{\partial z} & 0 & \frac{\partial}{\partial x} \\ \frac{\partial}{\partial y} & \frac{\partial}{\partial x} & 0 \end{bmatrix} \tag{10}$$

So using Equation-8 in Equation-9, the strain-nodal displacement relationship can be written as

$$\{\epsilon\} = [L]\{U\} = [L][N_U]\{U^e\} = [\bar{B}]\{U^e\} \tag{11}$$

where $[\bar{B}]$ matrix is strain-displacement matrix. Similarly Magnetic field $\{H\}$ can be written as

$$H = \begin{Bmatrix} H_x \\ H_y \\ H_z \end{Bmatrix} \tag{12}$$

where $H_x(x,y,z,t), H_y(x,y,z,t)$ and $H_z(x,y,z,t)$ are the magnetic field component in x, y and z direction respectively. These magnetic fields are obtained from element nodal magnetic fields $\{H^e\}(t)$, through the shape function, $[N_H(x,y,z)]$ as

$$\{H\} = [N_H]\{H^e\} \tag{13}$$

These would lead to the associated stiffness, mass and coupling matrices in terms of nodal displacements and nodal magnetic fields on minimizing the total energy using Hamilton's Principle . The details of these formulations are summarized below.

Strain Energy in magnetostrictive material is

$$\begin{aligned} V_e &= \frac{1}{2}\int \epsilon^T \sigma dv = \frac{1}{2}\int \epsilon^T\{[Q]\epsilon - [e]^T H\}dv = \frac{1}{2}\int \epsilon^T[Q]\epsilon dv - \frac{1}{2}\int \epsilon^T[e]^T H dv \\ &= \frac{1}{2}\int \{[\bar{B}]\{U^e\}\}^T[Q][\bar{B}]\{U^e\}dv - \frac{1}{2}\int \{[\bar{B}]\{U^e\}\}^T[e]^T[N_H]\{H^e\}dv \\ &= \frac{1}{2}\{U^e\}^T\int [\bar{B}]^T[Q][\bar{B}]dv\{U^e\} - \frac{1}{2}\{U^e\}^T\int [\bar{B}]^T[e]^T[N_H]dv\{H^e\} \\ &= \frac{1}{2}\{U^e\}^T\left[K_{UU}\right]\{U^e\} - \frac{1}{2}\{U^e\}^T\left[K_{UH}\right]\{H^e\} \end{aligned} \tag{14}$$

where $\{U^e\}$ and $\{H^e\}$ are nodal mechanical and magnetic degrees of freedom. K_{UU} is stiffness matrix for mechanical-mechanical degrees of freedom and K_{UH} is stiffness matrix for mechanical-magnetic degrees of freedom.

Kinetic Energy in magnetostrictive material is

$$\begin{aligned} T_e &= \frac{1}{2}\int \{\dot{U}\}^T[\rho]\{\dot{U}\}dv = \frac{1}{2}\int \{[N_U]\{\dot{U}^e\}\}^T[\rho][N_U]\{\dot{U}^e\}dv \\ &= \frac{1}{2}\{\dot{U}^e\}^T\int [N_U]^T[\rho][N_U]dv\{\dot{U}^e\} = \frac{1}{2}\{\dot{U}^e\}^T\left[M_{UU}\right]\{\dot{U}^e\} \end{aligned} \tag{15}$$

where $\{\dot{U}\}$ is velocity vector, ρ is density of the magnetosrictive material, $\{\dot{U}^e\}$ are nodal velocity of mechanical degree of freedom. M_{UU} is mass matrix for mechanical-magnetic degrees freedom.

Magnetic Potential Energy in magnetostrictive material is

$$\begin{aligned} V_m &= \frac{1}{2}\int B^T H dv \\ &= \frac{1}{2}\int \{[e]\epsilon + [\mu^\epsilon]H\}^T H dv \\ &= \frac{1}{2}\int \epsilon^T[e]^T H dv + \frac{1}{2}\int H^T[\mu^\epsilon]^T H dv \\ &= \frac{1}{2}\int \{[\bar{B}]\{U^e\}\}^T[e]^T[N_H]\{H^e\}dv + \frac{1}{2}\int \{[N_H]\{H^e\}\}^T[\mu^\epsilon]^T[N_H]\{H^e\}dv \\ &= \frac{1}{2}\{U^e\}^T\int [\bar{B}]^T[e]^T[N_H]dv\{H^e\} + \frac{1}{2}\{H^e\}^T\int [N_H]^T[\mu^\epsilon]^T[N_H]dv\{H^e\} \\ &= \frac{1}{2}\{U^e\}^T[K_{UH}]\{H^e\} + \frac{1}{2}\{H^e\}^T[K_{HH}]\{H^e\} \end{aligned} \tag{16}$$

where $[K_{HH}]$ is stiffness matrix of magnetic-magnetic degrees of freedom, $\{H^e\}$ is magnetic nodal degrees of freedom.

Magnetic External Workdone for N turn coil with coil current I is

$$\begin{aligned} W_m &= IN\int\{[\mu^\sigma]\{H\}\}.dA \\ &= In\int\{l_c\}^T[\mu^\sigma]\{H\}dv \\ &= In\{l_c\}^T\int[\mu^\sigma][N_H]\{H^e\}dv \\ &= In\{l_c\}^T\int[\mu^\sigma][N_H]dv\{H^e\} \\ &= \{F_H\}^T\{H^e\} \end{aligned} \tag{17}$$

where n is coil turn per unit length of coil and A is cross sectional area of the magnetostrictive material. l_c is the direction cosine of the coil axis.

$$\begin{aligned} K_{UU} &= \int[\bar{B}]^T[Q][\bar{B}]dv \\ K_{UH} &= \int[\bar{B}]^T[e]^T[N_H]dv \\ M_{UU} &= \int[N_U]^T[\rho][N_U]dv \\ K_{HU} &= \int[N_H]^T[e][\bar{B}]dv = {K_{UH}}^T \\ K_{HH} &= \int[N_H]^T[\mu^\epsilon]^T[N_H]dv \\ F_H &= In\{l_c\}^T\int[\mu^\sigma][N_H]dv \end{aligned} \tag{18}$$

Mechanical External Workdone is

$$\begin{aligned} W_e &= \int b^TUdv + \int\tau^TUdA \\ &= \{R\}^T\{U^e\} \end{aligned} \tag{19}$$

where b is body force. and τ is surface force, $\{R\}^T$ is equivalent nodal load for external mechanical forces of the magnetostrictive material.

3.1. Adaptive Analysis

Using Hamilton's Principle $\partial(\int_{t_1}^{t_2}(T_e - V_e + V_m + W_m + W_e)dt) = 0$ we get the following governing equation and its associated force boundary conditions.

3.1.1. Uncoupled Model In uncoupled model magnetic field, H is considered independent of mechanical condition [8] as

$$H = k_cI \tag{20}$$

Where K_c is coil constant. Hence in uncoupled model only mechanical degrees of freedom, U^e is unknown. Putting Hamiltonian's Equation the governing equation related to mechanical degrees of freedom is

$$[M_{UU}]\{\ddot{U^e}\} + [K_{UU}]\{U^e\} = [K_{UH}]\{H^e\} - \{R\} \tag{21}$$

Where H_e is calculated using Equation-20.

3.1.2. Coupled Model Unlike Uncoupled model, in coupled model mechanical and magnetic degree's of freedom is consider as unknown. Hence Hamiltonian's principle gives following Equations.

$$\begin{bmatrix} M_{UU} & 0 \\ 0 & 0 \end{bmatrix} \begin{Bmatrix} \ddot{U^e} \\ \ddot{H^e} \end{Bmatrix} + \begin{bmatrix} K_{UU} & -K_{UH} \\ K_{HU} & K_{HH} \end{bmatrix} \begin{Bmatrix} U^e \\ H^e \end{Bmatrix} = \begin{Bmatrix} -R \\ F_H \end{Bmatrix} \tag{22}$$

Note that generalized stiffness matrix is not symmetric matrix. Both the equations, sensing and actuation are coupled through the off-diagonal, sub-matrix of the stiffness matrix. Expanding Equation-22, we get

$$[M_{UU}]\{\ddot{U^e}\} + [K_{UU}]\{U^e\} - [K_{UH}]\{H^e\} = -R \tag{23}$$

and

$$\begin{aligned} [K_{UH}]^T\{U^e\} + [K_{HH}]\{H^e\} &= \{F_H\}^T \\ or \quad \{H^e\} &= [K_{HH}]^{-1}\{\{F_H\}^T - [K_{UH}]^T\{U^e\}\} \end{aligned} \tag{24}$$

Substituting $\{H^e\}$ from Equation-(24) in Equation-(23) we get

$$[M_{UU}]\{\ddot{U^e}\} + [K_{UU}{}^\star]\{U^e\} = \{F^\star\} \tag{25}$$

Where

$$\begin{aligned} [K_{UU}{}^\star] &= [[K_{UU}] + [K_{UH}][K_{HH}]^{-1}[K_{UH}]^T] \\ \{F^\star\} &= [K_{UH}][K_{HH}]^{-1}\{F_H\} - \{R\} \end{aligned} \tag{26}$$

Here all the stiffnesses can be calculated from Equation-(18).

3.2. Sensor Open Circuit Voltage

After determining the mechanical and magnetic degrees of freedom, sensor open circuit voltage can be post process in both coupled and uncoupled model. The sensor coil current is considered equal to zero. Using Faraday's law, open circuit voltage V in the sensing coil can be calculated from magnetic flux passing through the sensing patch.

3.2.1. Coupled Model Magnetic flux density is obtained from nodal magnetic field, which is obtained from finite element analysis. Thus open circuit voltage in the sensor can be calculated

as

$$\begin{aligned} V &= -N_s \int \frac{\partial}{\partial t}\{\mu^\sigma H\}.dA = -n_s\{l_c\}^T \int \frac{\partial}{\partial t}\{\mu^\sigma H\}dv \\ &= -n_s\{l_c\}^T \frac{\partial}{\partial t}\int \{\mu^\sigma H\}dv = -n_s\{l_c\}^T \int \{[\mu^\sigma][N_H]\}dv \;\; \frac{\partial}{\partial t}\{H_e\} \\ &= n_s\{l_c\}^T [\int \{\mu^\sigma[N_H]\}dv \;\; [K_{HH}]^{-1}[K_{UH}]^T]\frac{\partial}{\partial t}\{U^e\} \\ &= \{F_v\}^T\{\dot{U}^e\} \end{aligned} \tag{27}$$

where N_s is total coil turn and n_s is coil turn per unit length of the sensing patch. l_c is the direction cosine of coil axis and $\{\dot{U}^e\}$ is nodal velocity. $\{F_v\}^T$ is

$$\{F_v\}^T = n_s\{l_c\}^T \int \{\mu^\sigma[N_H]\}dv \;\; [K_{HH}]^{-1}[K_{UH}]^T \tag{28}$$

3.2.2. Uncoupled Model In uncoupled model, nodal magnetic field is zero as per Equation-20 with zero sensor coil current. To get open circuit voltage according to uncoupled model, magnetic flux density can be expressed in term of strain from sensing equation as

$$B = [d]\{\sigma\} = [d][Q]\{\epsilon\} = [e]\{\epsilon\} = [e][\bar{B}]\{U^e\} \tag{29}$$

Now using Faraday's law, open circuit voltage of the sensor can be calculated as

$$\begin{aligned} V &= -N_s \int \frac{\partial}{\partial t}[d]\{\sigma\}.dA = -n_s\{l_c\}^T \int \frac{\partial}{\partial t}[d]\{\sigma\}dv \\ &= -n_s\{l_c\}^T \frac{\partial}{\partial t}\int [e]\{\epsilon\}dv = -n_s\{l_c\}^T \frac{\partial}{\partial t}\int \{[e][\bar{B}]dv\{U^e\}\} \\ &= \{F_v\}^T\{\dot{U}^e\} \end{aligned} \tag{30}$$

And $\{F_v\}^T$ for uncoupled model is

$$\{F_v\}^T = -n_s\{l_c\}^T \int [e][\bar{B}]dv \tag{31}$$

4. Numerical Examples

Here we considered two examples - first is 1-D rod model to demonstrate the effect of coupling on the over all response. The next example explores the use of this material in composite beam using first order shear deformation theory.

4.1. One Dimensional Axial Element

To demonstrate the effect of coupling, the above 3-D Equations-(23,24) is reduced to simple 1-D model with mechanical displacement field (u, v, w) as

$$u(x, y, z, t) = u(x); \qquad v = 0; \qquad w = 0 \tag{32}$$

and magnetic field H as

$$H_x(x,y,z,t) = H(x); \quad H_y(x,y,z,t) = 0; \quad H_z(x,y,z,t) = 0 \tag{33}$$

for a magnetostrictive rod of length L, cross sectional area A, modulus of Elasticity E, magneto-mechanical strain coefficient d and constant stress permeability μ^σ. For finite element formulation, we use the conventional interpolation function that is, $u(x) = a_0 + a_1 x$, which gives the two shape functions as $N_1 = [1 - x/L]$ and $N_2 = [x/L]$. Hence displacement field can be written as

$$u(x) = N_1(x)u_1 + N_2(x)u_2 \qquad H(x) = N_1(x)H_1 + N_2(x)H_2 \tag{34}$$

Where u_1, u_2 are the element nodal displacement and H_1, H_2 are nodal magnetic fields. So both mechanical and magnetic shape function are considered as

$$[N_U] = [N_H] = \left[1 - \frac{x}{L} \quad \frac{x}{L}\right] \tag{35}$$

Using Equation-11, the strain-displacement matrix can be written as

$$\bar{B} = \left[-\frac{1}{L} \quad \frac{1}{L}\right] \tag{36}$$

Where strain $\epsilon = \frac{\partial u}{\partial x}$. The stiffness matrices can be calculated from Equation-18 as

$$[k_{UU}] = A\int_0^L \begin{bmatrix} -\frac{1}{L} \\ \frac{1}{L} \end{bmatrix} E \left[-\frac{1}{L} \quad \frac{1}{L}\right] dx = \frac{AE}{L}\begin{bmatrix} 1 & -1 \\ -1 & 1 \end{bmatrix} \tag{37}$$

$$[k_{UH}] = A\int_0^L \begin{bmatrix} -\frac{1}{L} \\ \frac{1}{L} \end{bmatrix} dE \left[1 - \frac{x}{L} \quad \frac{x}{L}\right] dx = \frac{AdE}{2}\begin{bmatrix} -1 & -1 \\ 1 & 1 \end{bmatrix} \tag{38}$$

$$\{F_H\} = InA\int_0^L \mu^\epsilon \left[1 - \frac{x}{L} \quad \frac{x}{L}\right]^T dx = \frac{I\mu^\sigma ALn}{2}\begin{bmatrix} 1 \\ 1 \end{bmatrix} \tag{39}$$

$$[k_{HH}] = A\int_0^L \begin{bmatrix} 1 - \frac{x}{L} \\ \frac{x}{L} \end{bmatrix} \mu^\epsilon \left[1 - \frac{x}{L} \quad \frac{x}{L}\right] dx = \frac{AL\mu^\epsilon}{6}\begin{bmatrix} 2 & 1 \\ 1 & 2 \end{bmatrix} \tag{40}$$

$$[F_v] = -n_s AEd\int_0^L \begin{bmatrix} -\frac{1}{L} \\ \frac{1}{L} \end{bmatrix} dx = -n_s AEd\begin{bmatrix} -1 \\ 1 \end{bmatrix} \tag{41}$$

4.1.1. Uncoupled Analysis For static uncoupled analysis corresponding equations are

$$\frac{AE}{L}\begin{bmatrix} 1 & -1 \\ -1 & 1 \end{bmatrix}\begin{bmatrix} u_1 \\ u_2 \end{bmatrix} - \frac{AdE}{2}\begin{bmatrix} -1 & -1 \\ 1 & 1 \end{bmatrix}\begin{bmatrix} H_1 \\ H_2 \end{bmatrix} = \begin{bmatrix} R_1 \\ R_2 \end{bmatrix} \tag{42}$$

Where $H_1 = H_2 = nI$ as per Equation-20 considering $k_c = n$.

- Keeping mechanically fixed boundary condition, $u_1 = u_2 = 0$ the blocked force in the support is

$$R_1 = -R_2 = AdEH_1 = AdEIn \tag{43}$$

- For mechanically free boundary condition, where $R_1 = R_2 = 0$ ($u_1 = 0$ to remove rigid body displacement).

$$u_2 = LdnI \tag{44}$$

- For sensor with tensile force F and zero coil current ($I = 0$), where $-R_1 = R_2 = F$ ($u_1 = 0$ to remove rigid body displacement).

$$H_1 = H_2 = 0 \qquad u_2 = \frac{FL}{AE} \qquad B = \frac{dEu_2}{L} = \frac{dF}{A} = d\sigma \tag{45}$$

Stress $\sigma = \frac{F}{A}$ which satisfies equilibrium equation.

4.1.2. Coupled Analysis For static coupled analysis corresponding equations are

$$\frac{AE}{L}\begin{bmatrix} 1 & -1 \\ -1 & 1 \end{bmatrix}\begin{bmatrix} u_1 \\ u_2 \end{bmatrix} - \frac{AdE}{2}\begin{bmatrix} -1 & -1 \\ 1 & 1 \end{bmatrix}\begin{bmatrix} H_1 \\ H_2 \end{bmatrix} = \begin{bmatrix} R_1 \\ R_2 \end{bmatrix} \tag{46}$$

$$\frac{AdE}{2}\begin{bmatrix} -1 & 1 \\ -1 & 1 \end{bmatrix}\begin{bmatrix} u_1 \\ u_2 \end{bmatrix} + \frac{AL\mu^\epsilon}{6}\begin{bmatrix} 2 & 1 \\ 1 & 2 \end{bmatrix}\begin{bmatrix} H_1 \\ H_2 \end{bmatrix} = \frac{I\mu^\sigma ALn}{2}\begin{bmatrix} 1 \\ 1 \end{bmatrix} \tag{47}$$

- Keeping mechanically fixed boundary condition, $u_1 = u_2 = 0$, the nodal magnetic field is

$$H_1 = H_2 = In\frac{\mu^\sigma}{\mu^\epsilon} \tag{48}$$

which is less than the generally considered value (In) for uncoupled model. Similarly the blocked force in the support is

$$R_1 = -R_2 = AdEH_1 = AdEIn\frac{\mu^\sigma}{\mu^\epsilon} \tag{49}$$

which is less than the value generally considered ($AdEIn$).

- For mechanically free boundary condition, where $R_1 = R_2 = 0$ ($u_1 = 0$ to remove rigid body displacement).

$$H_1 = H_2 = H = In \qquad u_2 = LdH \tag{50}$$

Stress $\sigma = E\frac{u_2}{L} - EdH = 0$ which satisfies equilibrium equation of free rod at mechanically free boundary condition.

- For sensor with tensile force F and zero coil current ($I = 0$), where $-R_1 = R_2 = F$ ($u_1 = 0$ to remove rigid body displacement).

$$H_1 = H_2 = -\frac{Fd}{A\mu^\sigma} \qquad u_2 = \frac{FL\mu^\epsilon}{AE\mu^\sigma} \qquad B = H\mu^\sigma = -\frac{Fd}{A} = -d\sigma \tag{51}$$

Stress $\sigma = \frac{F}{A}$ which satisfies equilibrium equation.

So It is clear that due to coupling, magnetic field and hence blocked force of a mechanically fixed rod is less than the value generally considered in uncoupled model. The ratio between these two values is calculated for terfenol-D rod taking data from Terfenol-D manual. Considering d=15E-9 m/amp, E=30GPa and constant stress relative permeability 10 for magnetostrictive material, $\frac{\mu^\sigma}{\mu^\epsilon} = 0.46$, which is around 50% of the value generally considered. However, for any other material if $\mu^\epsilon \gg d^2E$ then $\mu^\sigma = \mu^\epsilon$ and uncoupled and coupled model will give similar result. But for giant magnetostrictive materials like Terfenol-D, the effect of coupling stiffness matrix is considerable.

4.2. Cantilever Composite Beam

In this example, a cantilever beam modelled with the formulated elements having cross coupling stiffness is used to demonstrate the concept. Mechanical displacement fields are considered as

$$\begin{aligned} u(x,y,z,t) &= u^0(x,t) + z\theta_x^0(x,t) \\ v(x,y,z,t) &= 0 \\ w(x,y,z,t) &= w^0(x,t) \end{aligned} \tag{52}$$

where u, v, w are the components of mechanical displacement at location (x, y, z) in X, Y and Z direction respectively. u^0 and w^0 are the displacement components in mid plane of the composite beam. θ_x^0 is the angular rotation of the mid plane about X axis. Magnetic fields are

$$\begin{aligned} H_x(x,y,z,t) &= H_{xp}^0(x,t) \\ H_y(x,y,z,t) &= 0 \\ H_z(x,y,z,t) &= 0 \end{aligned} \tag{53}$$

where H_x, H_y and H_z are the component of magnetic fields at location (x, y, z) in X, Y and Z direction respectively. H_{xp}^0 is X directional magnetic field at mid plane of the magnetostrictive patch. So magnetic field along the thickness direction within the particular layer is considered as constant. In matrix notation Equation-52 can be written as

$$\{U\} = \begin{Bmatrix} u \\ v \\ w \end{Bmatrix} = \begin{bmatrix} 1 & 0 & -z \\ 0 & 0 & 0 \\ 0 & 1 & 0 \end{bmatrix} \begin{Bmatrix} u^0 \\ w^0 \\ \theta^0 \end{Bmatrix} = [N_p]\{\bar{U}\} \tag{54}$$

For finite element formulation, displacement and magnetic fields are discretise as

$$\begin{aligned} u^0(x) &= N_1(x)u_1 + N_2(x)u_2 \qquad & w^0(x) &= N_1(x)w_1 + N_2(x)w_2 \\ \theta^0(x) &= N_1(x)\theta_1 + N_2(x)\theta_2 \qquad & H(x) &= N_1(x)H_1 + N_2(x)H_2 \end{aligned} \tag{55}$$

Where u_1, u_2, w_1, w_2, θ_1, θ_2 are the element nodal displacements, slopes and H_1, H_2 are nodal magnetic fields. Equation-55 can be written in matrix form as

$$\{\bar{U}\} = [\bar{N}_U]\{U^e\} \qquad \{H\} = [N_H]\{H^e\} \tag{56}$$

Where nodal displacement vector, $\{U^e\}$ is

$$\{U^e\} = \{u_1 \;\; w_1 \;\; \theta_1 \;\; u_2 \;\; w_2 \;\; \theta_2\}^T \tag{57}$$

mechanical and magnetic shape functions are

$$[\bar{N}_U] = \begin{bmatrix} N_1 & 0 & 0 & N_2 & 0 & 0 \\ 0 & N_1 & 0 & 0 & N_2 & 0 \\ 0 & 0 & N_1 & 0 & 0 & N_2 \end{bmatrix} \qquad [N_H] = \begin{bmatrix} N_1 & N_2 \end{bmatrix} \tag{58}$$

where

$$[N_1] = \left[1 - \frac{x}{L}\right] \qquad [N_2] = \left[\frac{x}{L}\right] \tag{59}$$

To formulate mechanical shape function, mechanical displacement $\{U\}$ can be written as

$$\{U\} = [N_p][\bar{N}_U]\{U^e\} = [N_U]\{U^e\} \tag{60}$$

where mechanical shape function N_U is

$$[N_U] = \begin{bmatrix} N_1 & 0 & -zN_1 & N_2 & 0 & -zN_2 \\ 0 & 0 & 0 & 0 & 0 & 0 \\ 0 & N_1 & 0 & 0 & N_2 & 0 \end{bmatrix} \tag{61}$$

The strain displacement matrix B can be written from Equation-11 as follows

$$[B] = [L][N_U] = \begin{bmatrix} N_{1,x} & 0 & zN_{1,x} & N_{2,x} & 0 & zN_{2,x} \\ 0 & 0 & 0 & 0 & 0 & 0 \\ 0 & 0 & 0 & 0 & 0 & 0 \\ 0 & 0 & 0 & 0 & 0 & 0 \\ 0 & N_{1,x} & N_1 & 0 & N_{2,x} & N_2 \\ 0 & 0 & 0 & 0 & 0 & 0 \end{bmatrix} \tag{62}$$

From Equation-18 stiffness matrices and mass matrix can be computed. For simplification above strain-displacement matrix can be divided for axial, bending and shear parts of the energy as $[B] = [Ba] + z[Bb] + [Bs]$ respectively. Where Ba, Bb, Bs are as follows.

$$Ba = \frac{1}{L}\begin{bmatrix} -1 & 0 & 0 & 1 & 0 & 0 \\ 0 & 0 & 0 & 0 & 0 & 0 \\ 0 & 0 & 0 & 0 & 0 & 0 \\ 0 & 0 & 0 & 0 & 0 & 0 \\ 0 & 0 & 0 & 0 & 0 & 0 \\ 0 & 0 & 0 & 0 & 0 & 0 \end{bmatrix} \tag{63}$$

$$Bb = \frac{1}{L}\begin{bmatrix} 0 & 0 & -1 & 0 & 0 & 1 \\ 0 & 0 & 0 & 0 & 0 & 0 \\ 0 & 0 & 0 & 0 & 0 & 0 \\ 0 & 0 & 0 & 0 & 0 & 0 \\ 0 & 0 & 0 & 0 & 0 & 0 \\ 0 & 0 & 0 & 0 & 0 & 0 \end{bmatrix} \tag{64}$$

$$Bs = \frac{1}{L}\begin{bmatrix} 0 & 0 & 0 & 0 & 0 & 0 \\ 0 & 0 & 0 & 0 & 0 & 0 \\ 0 & 0 & 0 & 0 & 0 & 0 \\ 0 & 0 & 0 & 0 & 0 & 0 \\ 0 & -1 & L-x & 0 & 1 & x \\ 0 & 0 & 0 & 0 & 0 & 0 \end{bmatrix} \tag{65}$$

From Equation-18, stiffness matrix K_{UU} can be written as

$$\begin{aligned} K_{UU} &= \int [B]^T[Q][B]dv = \int [[Ba] + z[Bb] + [Bs]]^T[Q][[Ba] + z[Bb] + [Bs]]dv \\ &= \int [Ba]^T[Q][Ba]dv + 2\int [Ba]^T[Q][Bs]dv \\ &\quad + \int [Bs]^T[Q][Bs]dv + 2\int z[Ba]^T[Q][Bb]dv \\ &\quad +2\int z[Bs]^T[Q][Bb]dv + \int z^2[Bb]^T[Q][Bb]dv \\ &= [K_{UU}^{aa}] + [K_{UU}^{as}] + [K_{UU}^{ss}] + [K_{UU}^{ab}] + [K_{UU}^{sb}] + [K_{UU}^{bb}] \end{aligned} \tag{66}$$

To avoid shear locking, $[K_{UU}^{ss}]$ matrix is reduce integrated. These matrices are

$$[K_{UU}^{aa}] = \frac{1}{L}\begin{bmatrix} A_{11} & 0 & 0 & -A_{11} & 0 & 0 \\ 0 & 0 & 0 & 0 & 0 & 0 \\ 0 & 0 & 0 & 0 & 0 & 0 \\ -A_{11} & 0 & 0 & A_{11} & 0 & 0 \\ 0 & 0 & 0 & 0 & 0 & 0 \\ 0 & 0 & 0 & 0 & 0 & 0 \end{bmatrix} \tag{67}$$

$$[K_{UU}^{as}] = \frac{A_{15}}{2L}\begin{bmatrix} 0 & 2 & L & 0 & -2 & L \\ 2 & 0 & 0 & -2 & 0 & 0 \\ L & 0 & 0 & -L & 0 & 0 \\ 0 & -2 & -L & 0 & 2 & -L \\ -2 & 0 & 0 & 2 & 0 & 0 \\ L & 0 & 0 & -L & 0 & 0 \end{bmatrix} \tag{68}$$

$$[K_{UU}^{ss}] = A_{55}\begin{bmatrix} 0 & 0 & 0 & 0 & 0 & 0 \\ 0 & 1/L & 1/2 & 0 & -1/L & 1/2 \\ 0 & 1/2 & L/4 & 0 & -1/2 & L/4 \\ 0 & 0 & 0 & 0 & 0 & 0 \\ 0 & -1/L & -1/2 & 0 & 1/L & -1/2 \\ 0 & 1/2 & L/4 & 0 & -1/2 & L/4 \end{bmatrix} \tag{69}$$

$$[K_{UU}^{ab}] = \frac{B_{11}}{L}\begin{bmatrix} 0 & 0 & -1 & 0 & 0 & 1 \\ 0 & 0 & 0 & 0 & 0 & 0 \\ -1 & 0 & 0 & 1 & 0 & 0 \\ 0 & 0 & 1 & 0 & 0 & -1 \\ 0 & 0 & 0 & 0 & 0 & 0 \\ 1 & 0 & 0 & -1 & 0 & 0 \end{bmatrix} \tag{70}$$

$$[K_{UU}^{sb}] = \frac{B_{15}}{L}\begin{bmatrix} 0 & 0 & 0 & 0 & 0 & 0 \\ 0 & 0 & -1 & 0 & 0 & 1 \\ 0 & -1 & -L & 0 & 1 & 0 \\ 0 & 0 & 0 & 0 & 0 & 0 \\ 0 & 0 & 1 & 0 & 0 & -1 \\ 0 & 1 & 0 & 0 & -1 & L \end{bmatrix} \tag{71}$$

$$[K_{UU}^{bb}] = \frac{D_{11}}{L}\begin{bmatrix} 0 & 0 & 0 & 0 & 0 & 0 \\ 0 & 0 & 0 & 0 & 0 & 0 \\ 0 & 0 & 1 & 0 & 0 & -1 \\ 0 & 0 & 0 & 0 & 0 & 0 \\ 0 & 0 & 0 & 0 & 0 & 0 \\ 0 & 0 & -1 & 0 & 0 & 1 \end{bmatrix} \tag{72}$$

Where A_{ij}, B_{ij}, D_{ij} are

$$[A_{ij} \quad B_{ij} \quad D_{ij}] = \int \bar{Q}_{ij}[1 \quad z \quad z^2]dA \tag{73}$$

Similarly Mass matrix can be evaluate from Equation-15 as

$$[M_{UU}] = \frac{L}{6}\begin{bmatrix} 2I_0 & 0 & -2I_1 & I_0 & 0 & -I_1 \\ 0 & 2I_0 & 0 & 0 & I_0 & 0 \\ -2I_0 & 0 & 2I_2 & -I_1 & 0 & I_2 \\ I_0 & 0 & -I_1 & 2I_0 & 0 & -2I_1 \\ 0 & I_0 & 0 & 0 & 2I_0 & 0 \\ -I_1 & 0 & I_2 & -2I_1 & 0 & 2I_2 \end{bmatrix} \tag{74}$$

Where I_0, I_1, I_2 are the mass, first moment of mass and second moment of mass per unit length of the beam as

$$[I_0 \quad I_1 \quad I_2] = \int \rho[1 \quad z \quad z^2]dA \tag{75}$$

Considering $[e]$ matrix for beam element as

$$[e] = \begin{bmatrix} e_{11} & 0 & 0 & 0 & 0 & 0 \end{bmatrix} \tag{76}$$

Coupling stiffness matrix, K_{HU} can be calculated from Equation-14 as

$$[K_{HU}] = \frac{1}{2}\begin{bmatrix} -e_{11}^0 & 0 & e_{11}^1 & e_{11}^0 & 0 & -e_{11}^1 \\ -e_{11}^0 & 0 & e_{11}^1 & e_{11}^0 & 0 & -e_{11}^1 \end{bmatrix} \tag{77}$$

Where e_{11}^0 and e_{11}^1 are

$$[e_{11}^0 \;\; e_{11}^1] = \int e_{11}[1 \;\; z]dA \tag{78}$$

Similarly K_{HH} matrix can be written from Equation-18 as

$$[K_{HH}] = \frac{L\mu^0}{6}\begin{bmatrix} 2 & 1 \\ 1 & 2 \end{bmatrix} \tag{79}$$

Where μ^0 is

$$[\mu^0] = \int \mu^\epsilon dA \tag{80}$$

F_H matrix can be written as

$$[F_H] = \frac{In\mu^0 L}{2}\begin{bmatrix} 1 & 1 \end{bmatrix} \tag{81}$$

$\{F_v\}^T$ matrix can be written as

$$\{F_v\}^T = n\begin{bmatrix} e_{11}^0 & 0 & -e_{11}^1 & -e_{11}^0 & 0 & e_{11}^1 \end{bmatrix} \tag{82}$$

Numerical simulation is carried out by considering a unidirectional laminated composite beam of total thickness 1.8mm as shown in Figure-1. Length and width of the beam is 500mm and 50mm respectively. The beam is made of 12 layers with thickness of each layer being 0.15 mm. A numerical study on 12 layered beam containing two patches, one acting as an actuator and the other as a sensor has been presented. Numerical results have been given for a fixed position of sensor and actuator combination. Position of sensor is fixed at 9^{th} layer from bottom of the beam and near the support of the beam, whether the position of actuator is fixed at 1^{st} layer from bottom of the beam and 425 mm apart from support. Size of the actuator is 50mmX50mm with 0.15mm thickness and size of the sensor is 50mmX50mm with 0.3mm thickness. Elastic modulus of composite is 181 GPa and 10.3 GPa in parallel (E_1) and perpendicular (E_2) direction of fiber. Poison ratio (ν), density (ρ) and shear modulus (G_{12}) of composite is 0.0, 1.6 gm/c.c. and 28 GPa respectively. Elastic modulus (E_m), poison ratio (ν_m), shear modulus (G_m) and density (ρ_m) of magnetostrictive material is 30 GPa, 0.0, 23 GPa and 9.25 gm/c.c. respectively. Magneto-mechanical coupling coefficient is 15E-09 m/amp. Relative permeability μ_r is the ratio of permeability of the material and permeability of air. Permeability at vacuum or air is 400 π nano-Henry/m. Constant stress relative permeability of magnetostrictive material has been considered as 10. Number of coil turn in sensor (N) and actuator is 1000.

4.2.1. Static Analysis The effect of coupling of magnetostrictive material in composite beam for static actuation is analyzed with 1 Amp DC actuation coil current in the absence of sensor. It is observed that tip deflection for coupled analysis is 0.511mm, where as for uncoupled analysis 0.541mm. The ratio between these two is 1.06. As the thickness of the actuator is less compare to the thickness of the composite beam the effective increase of stiffness in the global stiffness matrix due to coupling is less. Increasing the thickness of actuator the effect on the ratio of coupled and uncoupled static tip deflection is shown in the Table-I. And here it is observed that the effect of coupling is increasing as the thickness of the actuator is increasing.

4.2.2. Time Domain Analysis To observe the effects of coupling terms of magnetostrictive material in dynamic analysis, time domain analysis is carried out with both low and high frequency actuation for the same cantilever composite beam. Here structure is actuated through time domain signal with actuation current I of 1 Amp at 50 Hz and 5kHz frequency. Actuation history for 5kHz signal is shown in Figure-2 with its frequency contents. Direct transient dynamic analysis has been done in 200 time steps to calculate open circuit voltage of the sensor and beam tip velocity in each time steps. Each time step is 50 mili-second and 5 micro-second for 50 Hz and 5kHz actuation respectively.

Figure-3 and Figure-4 shows the tip velocity of the cantilever beam for 50 Hz and 5kHz respectively. It is showing that unlike the static analysis, the effect of coupling in dynamic analysis is negligible. Moreover for high frequency actuation where effect of stiffness matrix is less than mass matrix, the effect of coupling is not observed.

Similar effect is observed in open circuit voltage in the sensor. Figure-5 and Figure-6 shows the open circuit voltage in the sensor for 50 Hz and 5kHz actuation respectively.

The effect of coupling on the thickness of the actuator with 50 Hz actuation frequency is shown in Figure-7 and Figure-8 and for tip velocity of the beam Figure-9 and Figure-10 for open circuit voltages.

Figure-11 and Figure-12 show the longitudinal magnetic field history and stress history along the length of the sensor respectively. According to uncoupled model magnetic field in the sensor is zero as current in sensor coil is zero. And as the stress along the sensor is different, according to uncoupled model magnetic flux in the different cross section along the length of the sensor will be different which is failing flux line continuity (Maxwell Equation $\nabla.B = 0$).

5. CONCLUSIONS

This study is mainly intended for the exploration of smart composite structures using a new FE formulation with magnetostrictive sensor and actuator considering their linear, coupled constitutive relationships. Coupled model is studied without assuming any direct relationship of magnetic field unlike uncoupled model. Here, elastic modulus, permeability and magneto-mechanical strain coefficient is considered as constant matrix. Actuation and sensing both has been done using actuation and sensing coil arrangement. Mechanical displacement and magnetic fields are considered as mechanical degrees freedoms and smart degrees of freedoms respectively for finite element formulation. Thus both sensor and actuator coil properties can be incorporated inside the finite element formulation. Through numerical simulation it has been shown that coupling stiffness matrix should be considered for the characterization of magnetostrictive rod. To demonstrate the concept, static and time domain analysis has been

performed for a 12 layer composite cantilever beam with magnetostrictive sensor and actuator considering smart degrees of freedom in the finite element analysis. It has been observed that the effect of coupling in static analysis is around 6%. and increasing with the thickness of the actuator. To observed the effect of coupling in the dynamic analysis both coupled and uncoupled analysis is carried out. It has been shown that the effect of coupling in dynamic analysis is less than static analysis. Specially for higher frequency actuation, the effect of coupling is negligible. If the thickness of the actuator increase the effect of coupling in the dynamic analysis also increase.

REFERENCES

1. Loewy, R.G. *Recent developments in smart structures with aeronautical applications*, Smart Materials and Structures, 6, 1997, pp. R11-R42.
2. Gandhi, M.V. and Jhompson, B.S. Smart Materials and Systems, Chapman and Hall, London 1992.
3. Brain, C. Smart Structures and materials, Artech house, Boston 1996.
4. E. Villery, *Change of magnetization by tension and by electric current.* Ann. Phys. Chem. 126 (1865), pp. 87-122.
5. Kleinke, D.K and Uras, H.M. A noncontacting magnetostrictive strain sensor, Rev. Sci. Instrum. 64, pp. 2361-2367, 1993.
6. Anjanappa, M., and Wu, Y. F. *Magnetostrictive particulate actuators: configuration, modeling and charaterization,* Smart Material and Structures, 6, 1997, pp. 393-402.
7. J N Reddy and J I Barbosa *On vibration suppression of magnetostrictive beams,* Smart Mater. Struct. 9 (2000) 49-58.
8. S.J. Lee, J.N. Reddy, F. Rostam-Abadi *Transient analysis of laminated composite plates with embedded smart-material layers* Finite Elements in Analysis and Design 40 (2004) 463483
9. Yoshiya Nakamura, Masanao Nakayama, Keiji Masuda, Kiyoshi Tanaka, Masashi Yasuda and Takafumi Fujita *Development of active six-degrees-of-freedom microvibration control system using giant magnetostrictive actuators.* Smart Mater. Struct. 9 (2000) 175-185.
10. I Pelinescu and B Balachandran *Analytical study of active control of wave transmission through cylindrical struts* Smart Mater. Struct. 10 (2001) 121-136
11. D. P. Roy Mahapatra, S. Gopalakrishnan, B. Balachandran; *Active feedback control of multiple waves in helicopter gearbox support struts.* Smart meterials and structures, 10(2001)1046-1058.
12. Ralph C Fenn, James R Downer, Dariusz A Bushko, Vijay Gondhalekar and Norman D Ham; *Terfenol-D driven flaps for helicopter vibration reduction* Smart Mater. Struct. 5 (1996) 49-57.
13. M Anjanappa and J Bi *Magnetostrictive mini actuators for Smart structures applications* Smart Mater. Struct. 3 (1994) 383-390.
14. Wu Qian, G R Liu, Lu Chun and K Y Lam *Active vibration control of composite laminated cylindrical shells via surface-bonded magnetostrictive layers* Smart Mater. Struct. 12 (2003) 889-897
15. M J Brennan, S J Elliott and R J Pinnington *A non-intrusive fluid-wave actuator and sensor pair for the active control of fluid-borne vibrations in a pipe* Smart Mater. Struct. 5 (1996) 281-296.
16. Krishna Murty, A. V., Anjanappa, M., Wang, Z. and Chen, X. *Sensing of delaminations in composite laminates using embedded magnetostrictive particle layers,* Journal of Intelligent Material Systems Structures, Vol-10 October 1999,pp 825-835
17. Saidha E., Naik G N and Gopalakrishnan, S. *An experimental investigation of a smart laminated composite beam with magnetostrictive patch for health monitoring applications.* Structural Health Minitoring.
18. Ghosh D. P. and Gopalakrishnan S., *Constitutive Relationships Of Magnetostrictive Material : Uncoupled Model.* communicated.
19. Ghosh D. P. and Gopalakrishnan S., *Role of Coupling terms in constitutive relationships of magnetostrictive materials.* Accepted in Computers, Materials, & Continua.
20. Mohamed E. H. Benbouzid, Gilbert Reyne, Gerard Meunier; *Nonlinear finite element modelling of giant magnetostriction.* IEEE transactions on magnetics, vol. 29, no. 6, November 1993.2467-2469.
21. Mohamed E. H. Benbouzid, Lars Kvarnsjo, Goran Engdahl; *Dynamic modelling of giant magnetostriction in terfenol-d rods by the finite element method.* IEEE transactions on magnetics, vol. 31 no. 3 May 1995.1821-1823
22. Mohamed E. H. Benbouzid, Gilbert Reyne, Gerard Meunier; *Finite element modelling of magnetostrictive*

devices: Investigations for the design of the magnetic circuit. IEEE transactions on magnetics, vol. 31, no. 3, May 1995.1813-1816
23. Butler, J.L, *Application manual for the design of Terfenol-D magnetostrictive transducers,* Edge Technologies Inc., Ames Iowa, 1988.

Table I. Vertical Displacement of Cantilever Tip

Thickness	Coupled	Uncoupled	Ratio
0.15mm	0.511mm	0.541mm	1.06
0.30mm	0.989mm	1.097mm	1.10
0.45mm	1.380mm	1.582mm	1.14
0.60mm	1.586mm	1.864mm	1.16

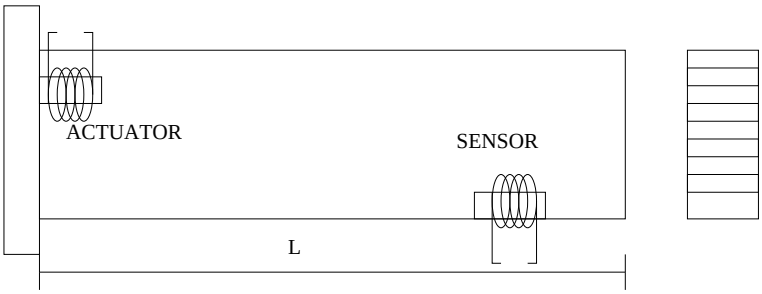

Figure 1. Laminated Beam With Actuator and Sensor.

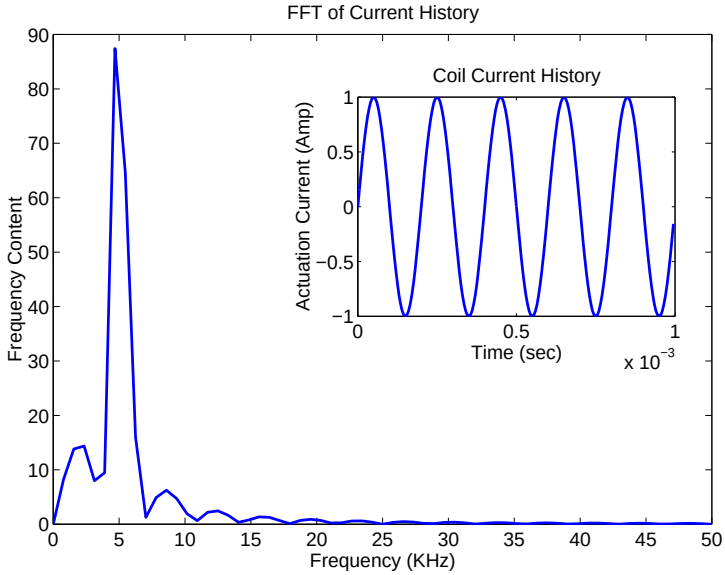

Figure 2. 5 kHz Actuation

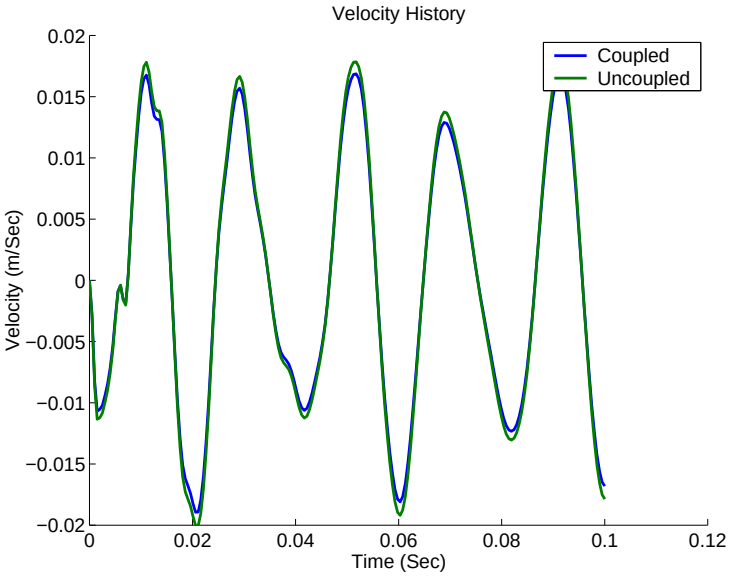

Figure 3. Tip Velocity for Coupled and Uncoupled analysis with for 50 Hz Actuation.

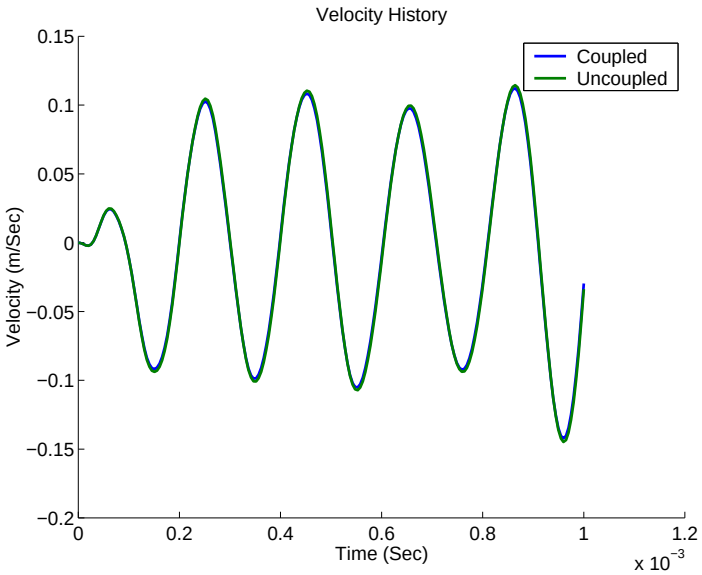

Figure 4. Tip Velocity for Coupled and Uncoupled analysis with 5kHz Actuation.

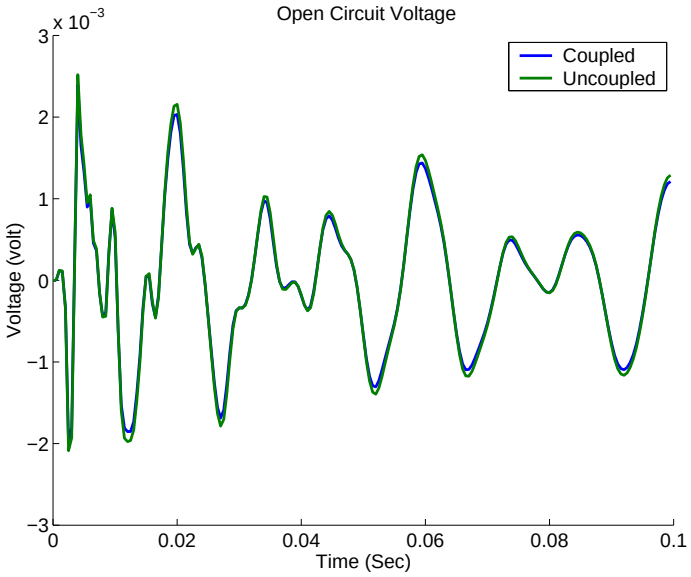

Figure 5. Open Circuit Voltage for Coupled and Uncoupled analysis with 50Hz Actuation.

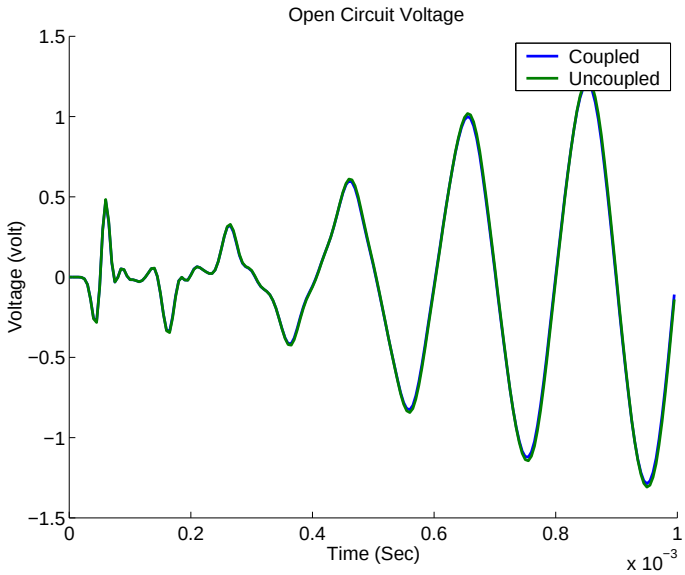

Figure 6. Open Circuit Voltage for Coupled and Uncoupled analysis with 5kHz Actuation.

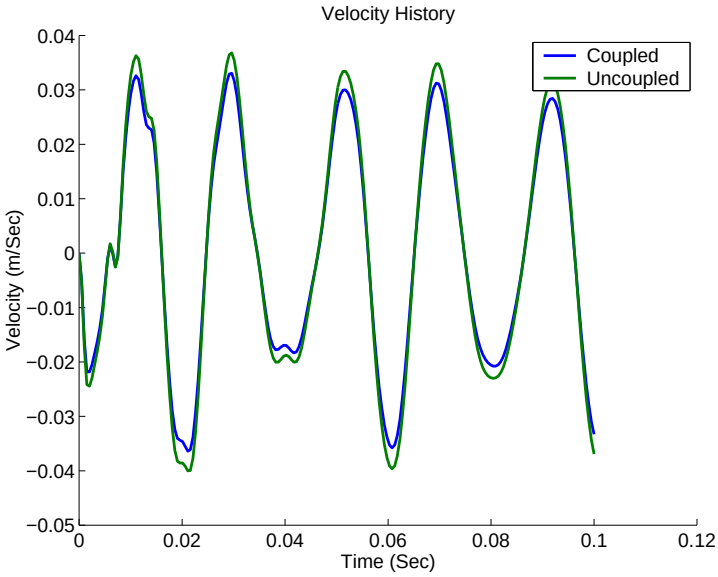

Figure 7. Cantilever Tip Velocity for Coupled and Uncoupled analysis with 0.3mm Actuator Thickness.

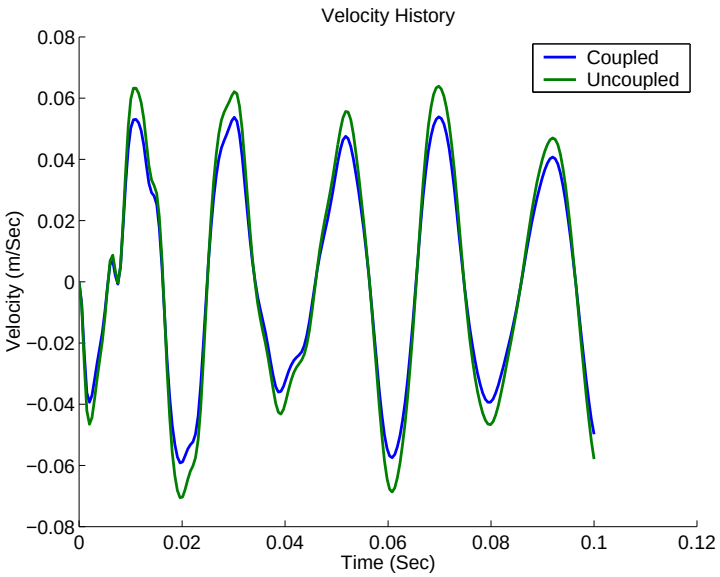

Figure 8. Cantilever Tip Velocity for Coupled and Uncoupled analysis with 0.6mm Actuator Thickness.

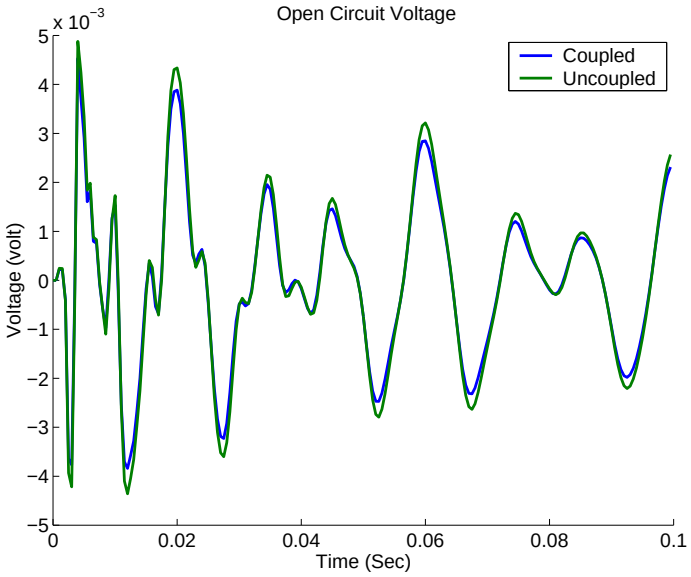

Figure 9. Open Circuit Voltage for Coupled and Uncoupled analysis with 0.3mm Actuator Thickness.

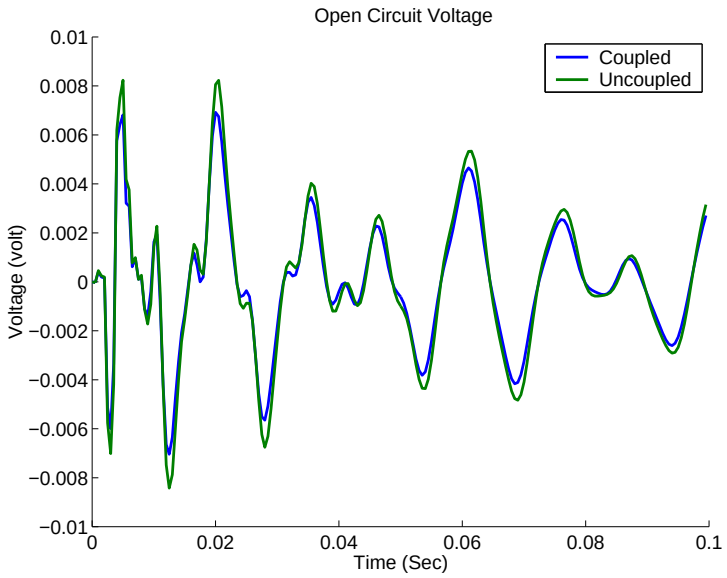

Figure 10. Open Circuit Voltage for Coupled and Uncoupled analysis with 0.6mm Actuator Thickness.

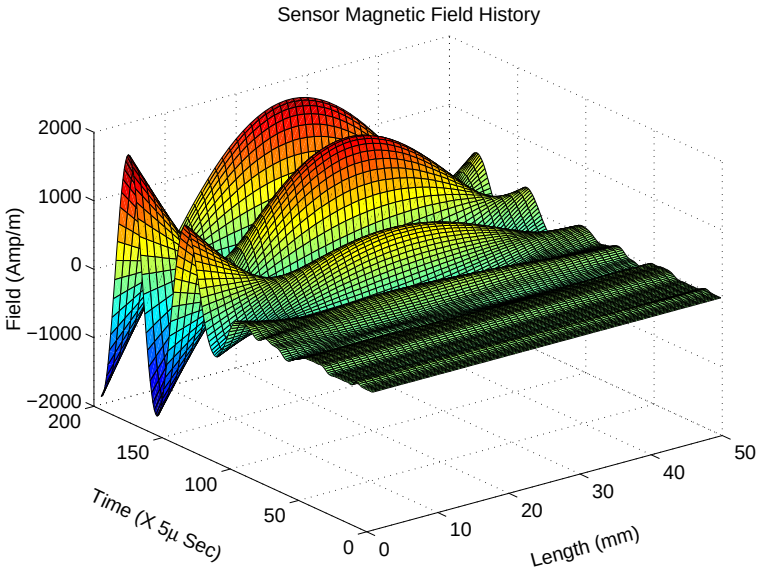

Figure 11.

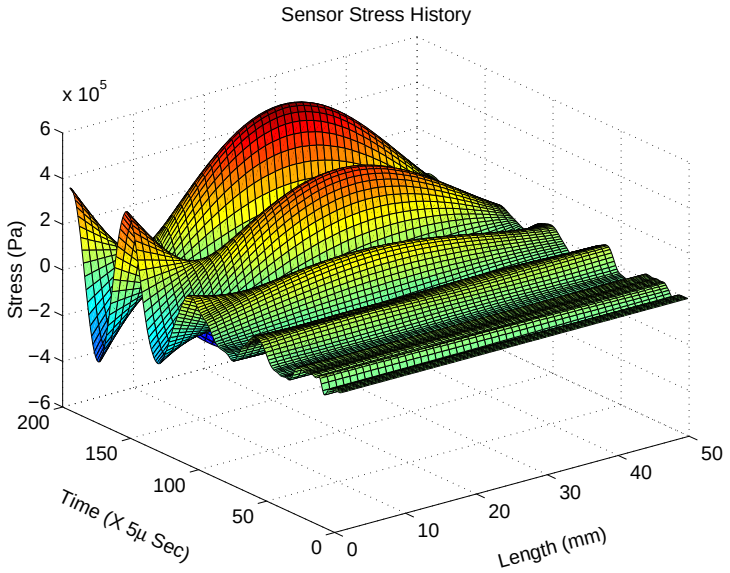
Sensor Stress History
x 10^5
6
4
2
0
−2
−4
−6
Stress (Pa)
200
150
100
50
0
Time (X 5μ Sec)
0
10
20
30
40
50
Length (mm)

Figure 12.